



Contents lists available at ScienceDirect

International Journal of Sediment Research

journal homepage: www.elsevier.com/locate/ijsrc

Q2 Original Research

Q7 Two-dimensional modeling of fine sediment transport with mixed sediment and consolidation: Application to the Gironde Estuary, France

Q6 Sylvain Orseau ^{a, b, *}, Nicolas Huybrechts ^{a, b}, Pablo Tassi ^{c, d}, Damien Pham Van Bang ^e, Fabrice Klein ^f^a Cerema, Direction Technique Eau, Mer et Fleuves, 134 rue de Beauvais, CS 60039-60280, Margny-lès-Compiègne, France^b Sorbonne Universités, Université de Technologie de Compiègne, CNRS, FRE2012 Roberval, Centre de Recherche Royallieu, CS 60 319, 60203, Compiègne Cedex, France^c Electricité de France, R&D Department, 6 quai Watier, BP 49, 78401, Chatou Cedex, France^d Laboratoire d'Hydraulique Saint Venant (ENPC-EDF/R&D-CEREMA), 6 quai Watier, BP 49, 78401 Chatou Cedex, France^e Centre Eau, Terre et Environnement, INRS-ETE, 490 rue de la Couronne, G1K 9A9, Québec (QC), Canada^f Grand Port Maritime de Bordeaux, 152 quai de Bacalan, CS 41320 – 33082, Bordeaux Cedex, France

ARTICLE INFO

Q3 Article history:

Received 18 December 2019

Accepted 24 December 2019

Available online xxx

Keywords:

Sediment transport
Morphodynamic model
Mixed sediment
Gironde Estuary
Opentelemac
Modeling system

ABSTRACT

In order to optimize ship navigation in the macrotidal Gironde Estuary, a recent project funded by the port of Bordeaux aims at better understand and forecast hydrodynamic and fine sediment transport within the estuary. In the framework of this project, a twodimensional hydro-sedimentary model is built. The model includes hydrodynamic forcings, mixed-sediment transport, and consolidation processes. The harmonic analysis of the astronomical tides reveals a strong distortion of the tidal wave inducing the growth of overtide constituents and the non-significant effect of tide-surge interactions in annual-scale prediction. Depending on hydrological conditions, river discharge can considerably alter the model accuracy due to the migration of the turbidity maximum zone modifying the bottom roughness. Comparison with measurements shows the ability of the model to reproduce suspended-sediment concentrations in the central Estuary. Sensitivity of the model to sediment features has also been discussed in regard of suspended-sediment concentrations and fluid mud deposits. The model will be further coupled with ship squat and morphodynamic models.

p { margin-bottom: 0.25 cm; line-height: 115%; }

© 2019 Published by Elsevier B.V. on behalf of International Research and Training Centre on Erosion and Sedimentation/the World Association for Sedimentation and Erosion Research.

1. Introduction

Located in the southwest of France, the Gironde Estuary is considered as the largest estuary in Western Europe (180 km in length and 20 km wide, Fig. 1). In the lower and central areas, the Gironde fluvial-estuarine system is characterized by a pronounced turbidity maximum zone (TMZ) that plays an important role in the sediment transport and morphodynamic of the study area (Jalón-Rojas et al., 2015; Sottolichio & Castaing, 1999). In such a highly turbid estuary (1–10 g/L near the bed), the maintenance of the

navigation channel is an important issue which arises with the growth of the ship capacity and the predominance of maritime transport. Under this context, Grand Port Maritime of Bordeaux (GPMB) has funded the Gironde XL 3D project, with the support of the European Union (EU). This project aims to develop numerical tools to safely accommodate larger ships by better anticipating channel maintenance requirements and operations. For both objectives, hydrodynamic and sediment transport models are needed over different time scales. On the one hand, the model should be able to predict in real time water levels, flow recirculation and concentrations of suspended particulate matter (SPM) over short periods of time (36 h) in order to maintain a safe under keel clearance for the ship navigation for given hydrological conditions. On the other hand, the annual time-scale must be considered for channel maintenance operations.

* Corresponding author. Cerema, Direction Technique Eau, Mer et Fleuves, 134 rue de Beauvais, CS 60039-60280, Margny-lès-Compiègne, France.

E-mail address: sylvain.orseau@tutanota.com (S. Orseau).

<https://doi.org/10.1016/j.ijsrc.2019.12.005>

1001-6279/© 2019 Published by Elsevier B.V. on behalf of International Research and Training Centre on Erosion and Sedimentation/the World Association for Sedimentation and Erosion Research.

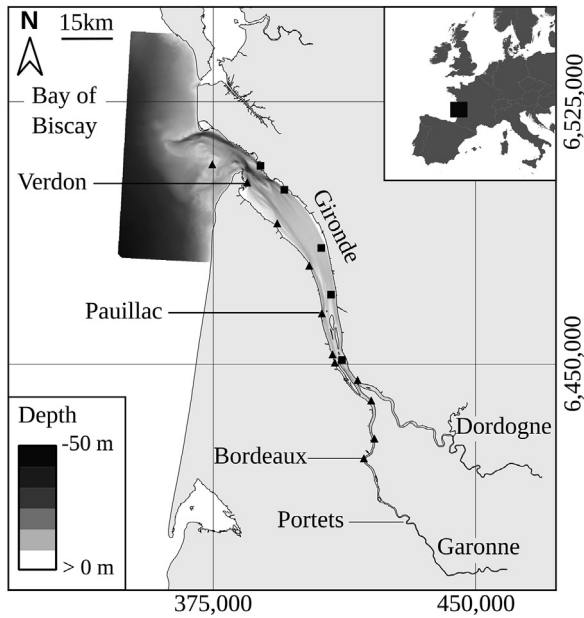


Fig. 1. Location map of the Gironde Estuary (France) and its main tributaries the Dordogne and the Garonne rivers. Measurement stations and tidal gages are represented along the estuary by black squares and black triangles, respectively. The bathymetric chart is computed with the inverse distance weight method and used data from surveys collected at different times from 2005 to 2018.

Over the years, several numerical models of the Gironde Estuary have been developed. The models can be grouped according to their usage with the first group mainly dedicated to hydrodynamics (Denot et al., 2000; Huybrechts et al., 2012; Laborie et al., 2014). The second group analyzes the turbidity maximum dynamics via three-dimensional models with a fixed bed configuration (Cancino & Neves, 1999; Diaz et al., 2018; Li et al., 1994; Sottolichio et al., 2001; van Maanen & Sottolichio, 2018). The last group focuses on two-dimensional, depth-averaged models (2DH) of sediment transport and bed evolution (Chini and Villaret, 2007; Huybrechts & Villaret, 2013; Van, 2012; Villaret et al., 2011). Huybrechts and Villaret (2013) simulated a 5 year morphodynamic evolution using three sand classes, while Villaret et al. (2011) and Van (2012) did numerical simulations considering cohesive sediment and bed consolidation.

The mouth of the estuary is mainly composed of sand (>90%) while a sand-mud mixture is observed in the intermediate estuary (75% of mud upstream the P2 station on Fig. 1 according to the GPMB). In the former area, some migrating sand banks also are observed (Kapsimalis et al., 2004). A 2DH modeling approach is selected here as a good compromise between computational cost and hydro-sedimentary processes. Compared to previous works (Huybrechts & Villaret, 2013; Van, 2012), a sand-mud approach is chosen in order to better reproduce the variability of the bed composition. In consequence, even if the model will also be used to predict bed evolution, this paper focuses on the development and the validation of a hydro-sedimentary model. In this way, the model must provide reliable predictions of water levels, current velocities, and SPM concentrations to further set up a Computational Fluid Dynamics (CFD) ship squat model (Ali et al., 2018). To the best of the authors knowledge, few models combining mixed sediment and consolidation processes have been applied for the Gironde Estuary.

This paper is organized as follows. In Section 2 the main features of the Gironde Estuary are briefly presented. In Section 3, the hydro-sedimentary mathematical model and its numerical solution

are introduced. In Section 4, numerical model calibration and validation are done for different hydrological conditions using measurements of water level, current velocity, salinity, and suspended-sediment concentration collected during the project. In Section 5, a sensitivity analysis for sediment parameters is done to improve the knowledge and the prediction of suspended-sediment concentrations in the Gironde Estuary. Ongoing studies also are discussed in the latter section.

2. Study area

The Gironde Estuary is a macrotidal and convergent estuary with a tidal range varying from 1.5 m during neap tides to 5.5 m during spring tides at the estuary mouth (Fig. 1). The propagation of the tide along the estuary induces an amplification of tidal waves and an asymmetry in the rise and fall of the water level with values of 4 h and 8 h 25 min, respectively. The limit of the tide propagation is located about 170 km upstream of the estuary mouth. Dordogne River and Garonne River contributions to the freshwater discharge are estimated to 35% and 65%, respectively (Sottolichio, 1999). For 2018, the total daily river discharge varied from 133 to 5560 m³/s⁻¹ during low and high river discharges periods, respectively. The annual volume of freshwater delivered to the sea is approximately 2.5 × 10¹⁰ m³. The highest velocities are observed in the navigation channel for the intermediate estuary and on the side channel for the lower estuary. Near the bottom, average current velocities are approximately equal to 0.75 m/s⁻¹ during spring tides and never exceed 0.5 m/s⁻¹ during neap tides (Castaing, 1981).

The Gironde Estuary is considered the largest estuary in Western Europe, with the width varying from 20 km at the estuary mouth to 3 km for the narrowest sections and with length of 70 km from the Bay of Biscay to the confluence of the Dordogne and Garonne rivers. Based on the bed composition, the estuary can be decomposed into 3 zones comprising (i) a sandy facies in the estuary mouth; (ii) a mixed facies dominated by mud (primarily composed of clays) along the central part, and (iii) a fluvial estuary, in the most upstream parts, characterized by the presence of sand, pebbles, and gravel (Jalón-Rojas et al., 2015; Mélières & Martin, 1969).

Fine suspended-sediment observed in the Gironde Estuary are mainly characterized (>90%) by sediment diameters smaller than 16 μm (Jouanneau & Latouche, 1981). A large part of these fine sediment composes a pronounced Turbidity Maximum Zone (TMZ) with concentrations ranging between 1 and 10 g/Li⁻¹ (Sottolichio & Castaing, 1999). The TMZ formation is mainly due to the tidal asymmetry and partly to the vertical density gradient which maintains suspended sediment in the TMZ (Allen, 1972; Castaing, 1981; Sottolichio et al., 2001). Its location along the estuary migrates between Portets and off the estuary mouth depending on hydrological conditions (Castaing, 1981; Jalón-Rojas et al., 2015).

3. Materials and methods

3.1. Mathematical models

Hydrodynamics processes are simulated using the continuity and momentum equations solve as the shallow water equations. This model includes parameterizations for the diffusion term and bottom friction. For further details, see Santoro et al. (2017). Bed composition is considered as a mixture of two sediment classes (sand and mud), characterized by their fraction and properties, such as the grain size, the settling velocity, and the concentration. The depth-averaged sediment concentration equation for suspended sediment transport is computed as follows:

$$\frac{\partial C}{\partial t} + U \frac{\partial C}{\partial x} + V \frac{\partial C}{\partial y} = \frac{1}{h} \left[\frac{\partial C}{\partial x} \left(h \varepsilon_x \frac{\partial C}{\partial x} \right) + \frac{\partial C}{\partial y} \left(h \varepsilon_y \frac{\partial C}{\partial y} \right) \right] + \frac{E - D}{h} \quad (1)$$

where C is the depth-averaged concentration of the size class of sediment, in kg/m^3 , U and V are the depth-averaged velocity component along the x and y directions, respectively, in m/s , h is the water depth in m , ε_x and ε_y are the diffusion coefficients along the x and y directions, respectively, in m^2/s . In Eq. (1), the net sediment flux equals the summation of sediment erosion flux E , kg/s/m^2 , and sediment deposition flux D , kg/s/m^2 , computed according to the Parthenadies (1965) and the Krone (1962) formulations, respectively.

The bed is discretized with a fixed number of layers in which each layer thickness and sand and mud classes are initialized at time $t = 0$. The state of consolidation is reckoned through a linear relationship between the critical shear stress for erosion of mud ($0.5 < \tau_{ce} < 1.5 \text{ N/m}^2$) and the mud concentration of each layer ($75 < C_{mud} < 500 \text{ g/L}$). Erosion constants, E_0 , are set constant for all layers. The critical shear stress for erosion (τ_{ce}) and the erosion rate are computed according to the mud fraction (f_m) (Waeles, 2005). To consider the influence of mixed sediments on bed properties, the authors compute erosion rates for mud (E_m) and sand (E_s) separately and depending to the regime type (cohesive, non-cohesive, or mixed). For non-cohesive ($f_m < 30\%$) and cohesive ($f_m > 50\%$) regimes, different formulations for the critical shear stress for erosion are used accounting for the sediment type (Eq. (2)).

$$E = f \cdot E_0 \cdot T^a \quad (2)$$

where depending on the sediment type (mud or sand), E_s and E_m are the erosion rates of sand and mud, $\text{kg/m}^2/\text{s}$, f is the proportion of sand or mud, between 0 and 1, E_{0s} and E_{0m} are the erosion constants of sand or mud, respectively, $\text{kg/m}^2/\text{s}$, $T = (\tau_b - \tau_{ce})/\tau_{ce}$ with τ_b the bottom shear stress, in kg/m/s^2 , τ_{ce} the critical shear stress for erosion, and a is a constant equal to 0.5. For the mixed regime ($30\% < f_m < 50\%$), a weighted average is used to compute the erosion rates of sand (Eq. (3)) and mud (Eq. (4)):

$$E_s = (1 - f_m) \left(E_{0s} + \frac{E_{0m} - E_{0s}}{f_{m,crit^*} - f_{m,crit}} (f_m - f_{m,crit}) \right) T^{a + \frac{1-a}{f_{m,crit^*} - f_{m,crit}} (f_m - f_{m,crit})} \quad (3)$$

$$E_m = f_m \left(E_{0m} + \frac{E_{0s} - E_{0m}}{f_{m,crit^*} - f_{m,crit}} (f_m - f_{m,crit}) \right) T^{a + \frac{1-a}{f_{m,crit^*} - f_{m,crit}} (f_m - f_{m,crit})} \quad (4)$$

Deposition fluxes of sand and mud are computed by including the deposition probabilities for each fraction in the Krone equation (Eq. (5)). For both classes, the settling velocity W_s is set to a constant equal to $7.5 \cdot 10^{-4} \text{ m/s}$. Following Le Hir et al. (2001) and van Maanen and Sottolichio (2018), a high critical shear velocity for deposition of mud is applied ($u_{cd}^* = 10 \text{ m/s}$). Sand and mud suspensions can, thus, occur during the whole tidal cycle.

$$D = \begin{cases} W_s C \left[\left(1 - \frac{u^*}{u_{cd}^*} \right)^2 \right] & \text{if } u^* < u_{cd}^* \\ D = 0 & \text{if } u^* > u_{cd}^* \end{cases} \quad (5)$$

where u^* is the shear velocity, m/s . Consolidation processes are accounted for with an iso-concentration multi-layer consolidation model for mixed sediment (Villaret et al., 2011; Villaret & Walther, 2008) that assumes that the vertical flux of sediment between

layers is proportional to the sediment mass in each layer, via the use of mass transfer coefficients. This approach was chosen to consider the sediment as a mixture in bed consolidation and differs from previous studies which include bed consolidation using the Gibson theory (Santoro et al., 2017; Thiebot et al., 2011; Van, 2012) with mud only. The bed is discretized with 20 layers characterized by a sediment concentration, a thickness, and a mass transfer coefficient set empirically to reproduce consolidation. During the simulation, only layer thicknesses vary and the mass balance computed for each layer is computed using Eq. (6).

$$\frac{M_i(t + \Delta t) - M(t)}{\Delta t} = F_i(t) - F_{i+1}(t) = -a_i M_i(t) \quad (6)$$

where i is the layer number, M_i is the mass per unit surface, kg/m^2 , F_i is the sediment flux at the lower boundary of the i -th layer, kg/s/m , and a_i is the mass transfer coefficient s^{-1} .

3.2. Model setup

Numerical computations are done using the open source Telemac-Mascaret system (www.opentelemac.org). Hydrodynamics are computed using the module TELEMAC-2D which solves the shallow water equations using the finite element method (Hervouet, 2007). This module is coupled at each time step with the module SISYPHE which solves the sediment transport and the bed evolution for both suspended and bedload transport processes. In the current study, only suspended sediment transport processes are considered. The domain is discretized with an unstructured triangular mesh of 27,000 nodes that spreads over an area of 2200 km^2 . The numerical domain extends over the entire estuary from the Bay of Biscay to the limit of the tide influence 170 km upstream from the estuary mouth. The study focuses on the intermediate estuary at the confluence of the Dordogne and Garonne rivers (Fig. 1). Inside this study area, cell lengths vary from 180 m and up to 300 m . Bathymetric data from 2009 to 2016 collected by the national hydrographic service (SHOM) and the GPMB has been interpolated on the mesh grid. The computational time requires 2 h to simulate 50 d with a time step of 10 s (using a work station with 12 cores of 2.4 GHz and 48 Go Ram).

Offshore boundary conditions are imposed from North East Atlantic (NEA) tidal atlases (Pairaud et al., 2008) including 46 harmonic constituents for better predictions of water levels (Huybrechts et al., 2012) and upstream boundary conditions are imposed from daily river discharges for both main tributaries. Mean sea level is obtained from the annual average of water levels collected at the Verdon station (Fig. 1) and defined at a value of 0.442 m . This latter value is then applied to the maritime boundary with also a constant salinity of 35 g/L and null values for the SPM. At upstream boundaries, fresh water is imposed while SPM values are taken from Jalón-Rojas et al. (2015).

The bottom friction is parameterized over 10 zones with a Strickler formulation, with roughness coefficients varying from 40 to $100 \text{ m}^{1/3}/\text{s}^{-1}$, obtained from the calibration of water levels and currents (Huybrechts et al., 2012; Ross et al., 2017). The lower value corresponds to sandy areas of the estuary mouth and is relatively close to the value predicted using the van Rijn formulation considering the bedform influence (Huybrechts et al., 2012; Van Rijn, 2007). Higher values of the bed friction imposed in the intermediate and upper estuaries correspond to flat muddy beds.

One of the main issues to deal with for mixed sediment (sand-mud or graded sand) is to impose the initial distribution of the mixture over the computational domain and for the bed structure. Due to lack of measurements, the initial distribution is numerically determined assuming a sandy bed (mean diameter = 0.4 mm) at the estuary mouth as suggested by Van (2012). At the intermediate

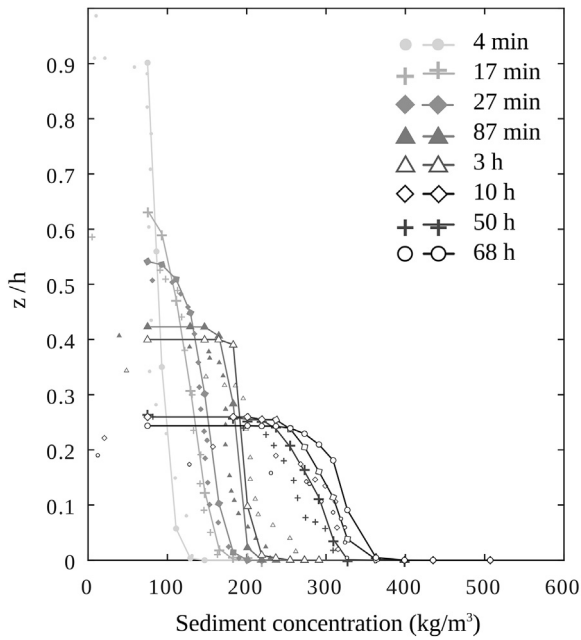


Fig. 2. Temporal evolution of the relative sediment height z/h (where z is the elevation above the channel bed) for vertical profiles of sediment mass concentration obtained from settling column experiments conducted by Van (2012) (markers) and the semi-empirical multi-layer model (line and markers).

estuary, the mud fraction is predominant in the bed composition with the presence of sand in some locations (Villaret et al. 2010). The bathymetry is defined by the port around 1200 kg/m³

(McAnally et al., 2016; Xu & Yuan, 2007), corresponding to a concentration layer of ~330 g/L. The fluid mud is initially provided on the navigation channel as proposed by Sottolichio (1999). It is distributed along the first five layers (from 75 to 147 g/L) over an area of 40 km² and has a thickness of the order of 0.5 m. A 2.5 m mud thickness is also distributed along layers from 237 to 500 g/L which corresponds to a more consolidated substrate below the bathymetry definition. Simulations are run without considering bed evolution, but the layers update in order to distribute the fluid mud along the estuary.

In order to simulate mud consolidation, a calibration procedure was applied to obtain the most representative temporal evolution of the sediment height and associated massive sediment concentrations (Fig. 2). Vertical profiles computed with the consolidation model are adjusted according to the values obtained from settling column experiments (Van, 2012). The maximum number of bed layers has been increased up to 20 layers in order to obtain a better discretization of the bed. Fair agreement between measured and computed values is obtained after the calibration of mass transfer coefficients for each layer. The values of the mass transfer coefficients and sediment concentrations vary from 3×10^{-3} to $1 \times 10^{-6} \text{ s}^{-1}$ and from 75 to 507 g/L⁻¹, respectively, over layers 1 to 20. These concentrations have been defined according to the experiments of Van (2012) and are in agreement with field observations in the Gironde Estuary (Abril et al., 2000) and other estuaries (McAnally et al., 2007a, b).

4. Numerical model calibration and validation

Numerical model calibration and validation are done by comparing measurements acquired during the project and

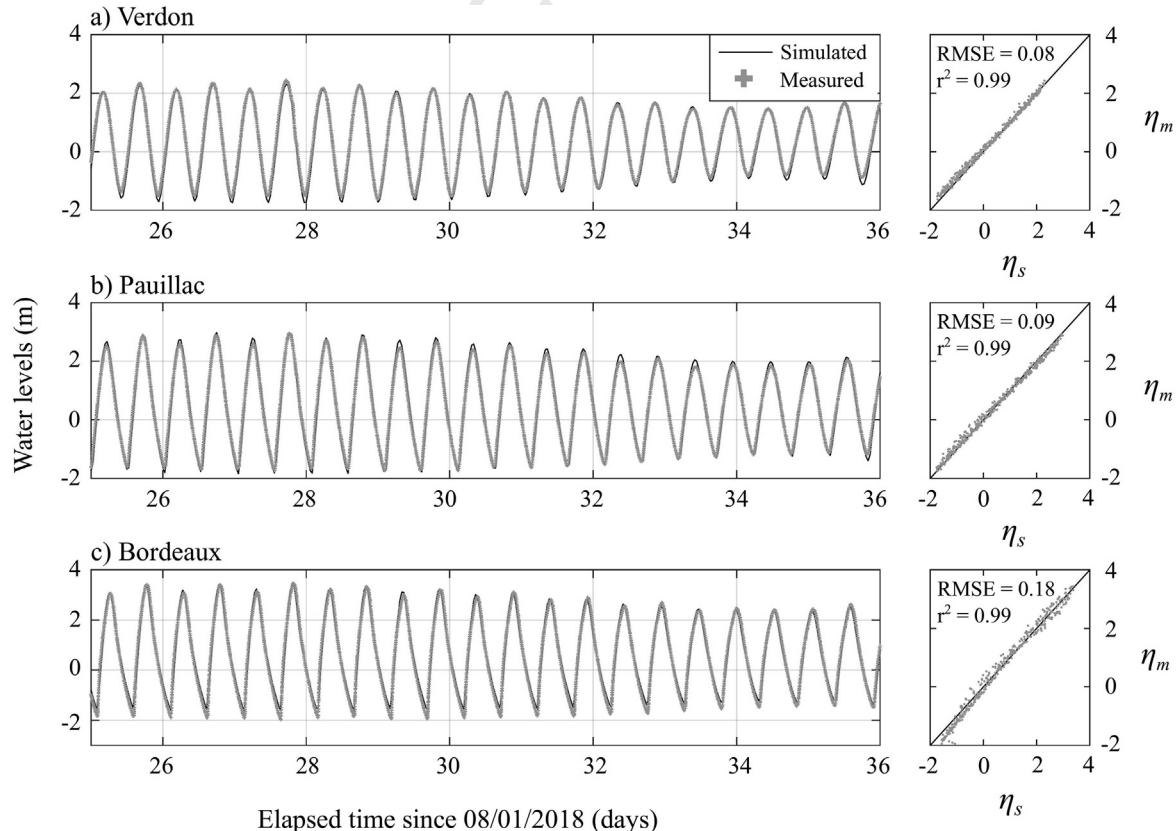


Fig. 3. Time series of simulated (black line) and measured (grey points) water levels at the (a) Verdon, (b) Pauillac, and (c) Bordeaux stations and their respective cross-validations. η_m and η_s correspond to the measured and the simulated free surface, respectively. The simulation is done during a low river discharge period (from August to September 2018).

simulated values for the following parameters: (i) water level; (ii) current velocity; (iii) salinity; and (iv) suspended-sediment concentration.

4.1. Water levels

Huybrechts et al. (2012) calibrated the bed friction coefficient of the model in order to make the water level difference between measured and simulated lower than 10 cm at the mouth and the central part of the estuary. The calibration and validation have been done for flow currents and water levels obtained during field investigations in August 2006 and October–November 2009. These two events were characterized by low river discharges and calm weather conditions. The hydrodynamic model only included river and tidal forcings. Ten years later, the morphodynamics of the Gironde Estuary may have changed. More recent bathymetric surveys have been performed and can be now considered in the model. It is, thus, necessary to check the validity of the calibration, then to analyze how the model behaves for different hydrological conditions in the upper estuary where the port terminals are located. The calibration update and validation of the hydrodynamics are realized during low (<200 m³/s) and high river discharges (between 1000 and 2000 m³/s) for neap and spring tide conditions.

During 15 days of low flow conditions (between 08/26 and 09/06/2018), the total river discharge varied from 161 to 235 m³/s⁻¹. Comparison between measured and computed water levels shows the ability of the model to predict the tidal amplitude, as well as, the tidal asymmetry with Root Mean Squared Error (RMSE) values up to 18 cm at the Bordeaux station (Fig. 3). Better results are found at the Verdon and Pauillac stations, in the lower and intermediate parts of the estuary (Fig. 1), with RMSEs below 10 cm. Maximum errors are mainly observed during high and low water conditions at the Bordeaux station in the upper estuary. Regression analysis shows a very good fit for every station with coefficients of determination, r², of 0.99 confirming the robustness of the model to predict water levels. However, these accurate predictions of the water level obtained during low river discharges could be degraded during flood periods. Indeed, seasonal variation of river discharges induces the migration of the turbidity maximum (Sottolichio, 1999) which can modify the estuarine bed texture and may have a significant impact on the bed friction (Jalón-Rojas et al., 2018).

Differences observed between measured and simulated water levels can come from two sources: a calibration using constant bed friction coefficients with hydrological conditions and/or variation of mean sea level due to tide-surge interactions. To distinguish the influence of the friction calibration and the impact of mean sea level on numerical results, harmonic analysis (Pawlowicz et al., 2002) is also performed on a longer time series at Verdon, Pauillac, and Bordeaux stations (Fig. 4). The lack of data for the year 2018 resulted in the harmonic analysis being done with water levels measured during 2015 over a period of 3 months. As expected, the analysis revealed the predominance of the M2 harmonic constituent (principal lunar semidiurnal) in the composition of the tidal amplitude for the predicted and measured values with values varying around 1.55 m (Fig. 4a). The N2 (larger lunar elliptic semidiurnal) and S2 (principal solar semidiurnal) constituent harmonics complete 90% of the signal with amplitudes around 0.3 m and 0.5 m, respectively. Moreover, the amplification of shallow water overtides M4 and M6 is noticed at upstream stations (Fig. 4b and c). Differences between measured and predicted values of amplitude are small and never exceed 7 cm for all harmonic constituents and for all stations. For semi-diurnal constituents (M2, N2, and S2) at the Verdon station, amplitude errors are below 5 cm with a maximum value for the M2 harmonic (4.2 cm).

Phase lags are also well reproduced with computed delays of 4 min and of less than a minute for M2 and S2 harmonics, respectively (Fig. 4d–f). For M4 and M6 harmonics delays increase up to 16 min. For overall harmonics, phase lags do not show significant variations during the tidal propagation. In summary, the harmonic analysis points out that differences in amplitude of the main tidal components are small. For two-dimensional (2D) modeling, this analysis supports the hypothesis of a seasonal calibration of the model. Trial and error methodology as done by Huybrechts et al. (2012) is not suitable to do regular updates of the bed friction calibration. Therefore, the application of automatic calibration and optimization procedures is more suitable (Smaoui et al 2018).

4.2. Current velocities

As also observed for water levels, the accuracy of current velocity predictions decreases in the upstream direction. According to Fig. 5a–b, results are good enough at Stations P1 and P4 with r² of 0.79 and 0.90, respectively. However, the robustness of the model decreases at Station P5 where simulations overestimate the strength of ebb currents, particularly during spring tides. For the latter conditions, the measurements describe a well-marked tidal asymmetry characterized by short flood tides and long ebb tides. However, at Station P5 where the measured asymmetry is the

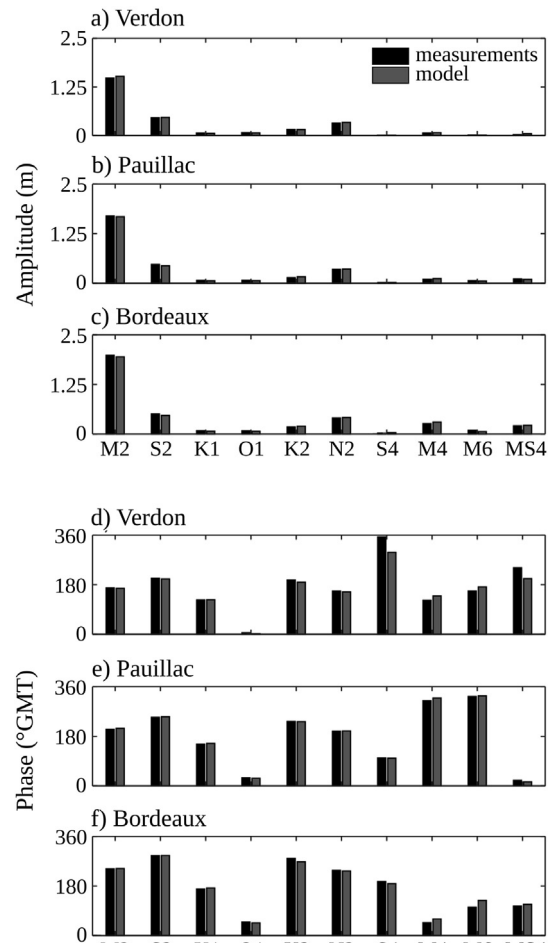


Fig. 4. Tidal harmonic analysis of measured (black) and simulated (grey) water level time series acquired during low river discharges in 2015. Water levels were collected at the Verdon (a, d), Pauillac (b, e), and Bordeaux (c, f) stations.

strongest, mean velocities of flood and ebb currents are equivalent and equal to 1 and 0.98 m/s, respectively (Fig. 5c). For the same station, the RMSE reaches the maximum value of 0.14 m/s which is not so high compared to other stations where the minimum value is 0.09 m/s. The best results are obtained at Station P1 where ebb currents are accurately predicted. For other stations, ebb currents are difficult to predict with an underestimation of the peak ebb velocity and an overall overestimation of velocities during the fall of the tide (Fig. 5b and c).

4.3. Salinity

Validation of salinity predictions used data collected near the bed during mooring surveys and for different hydrological conditions (see Section 4.3). The simulation started during neap tides characterized by low tidal amplitudes of measured salinity (below ~ 10 psu) for all stations (Fig. 6c–e). Conversely, maximum tidal amplitudes are observed during spring tides between days 9 and 13 with a maximum value of 17 psu. However, for the last half of the simulation, the overall salinity tends to decrease in response to a steep increase of the total river discharge of $821 \text{ m}^3/\text{s}$ in 6 d (Fig. 6b–d). Despite these changing conditions, the model correctly predicts tidal and fortnightly variations, but tends to underestimate the amplitude of tidal variations, particularly near the estuary mouth at station P1 (Fig. 6c). These differences ranging between 3.12 and 6.7 psu are mainly due to the fact that measurements are taken near the bed, while numerical values of salinity correspond to depth-averaged quantities.

A few kilometers upstream, at Station P2, the amplitude is better reproduced, particularly between days 8 and 12 (Fig. 6d). However,

for some tidal cycles, measured salinity shows rapid changes not captured by the numerical model. This observation could be explained by the presence of a strong vertical density gradient in this area which cannot be reproduced by 2DH model. In the intermediate estuary, at the Station P4, measured salinity decreases rapidly below 5 psu indicating that the salt intrusion limit is close under this hydrological condition (Fig. 6e). In this area, where salinity values are generally low but could increase considerably near the bed, the 2DH model is less accurate but still provides reliable predictions.

For the low river discharges period, the highest flowrates are observed between days 29 and 32 with a maximum value of $235 \text{ m}^3/\text{s}$ (Fig. 7b). In this hydrological condition, density stratification is weak and allows accurate predictions, particularly at Station P4 with $r^2 = 0.84$ (Fig. 7d). At Station P1, the model correctly predicts tidal variations of salinity but slightly overestimates salinity during slack waters with a difference up to 2.7 psu for both high and low water slacks, respectively (Fig. 7c). As observed for the flood period, surrounding areas of the salt intrusion limit, where salinity is low, are difficult to predict. At Station P5, conversely to the flood period, the model overestimates salinity, but measurements seem to be wrong and describe a linear signal since day 30 owing to the malfunctioning of the probe (Fig. 7e).

4.4. Suspended-sediment

In order to compare predicted and measured values, a correction factor estimated using a simplified Rouse profile has been applied. The Rouse profile was set using a linear increase of the vertical diffusivity and a reference altitude z_a of 1 m. During the flood

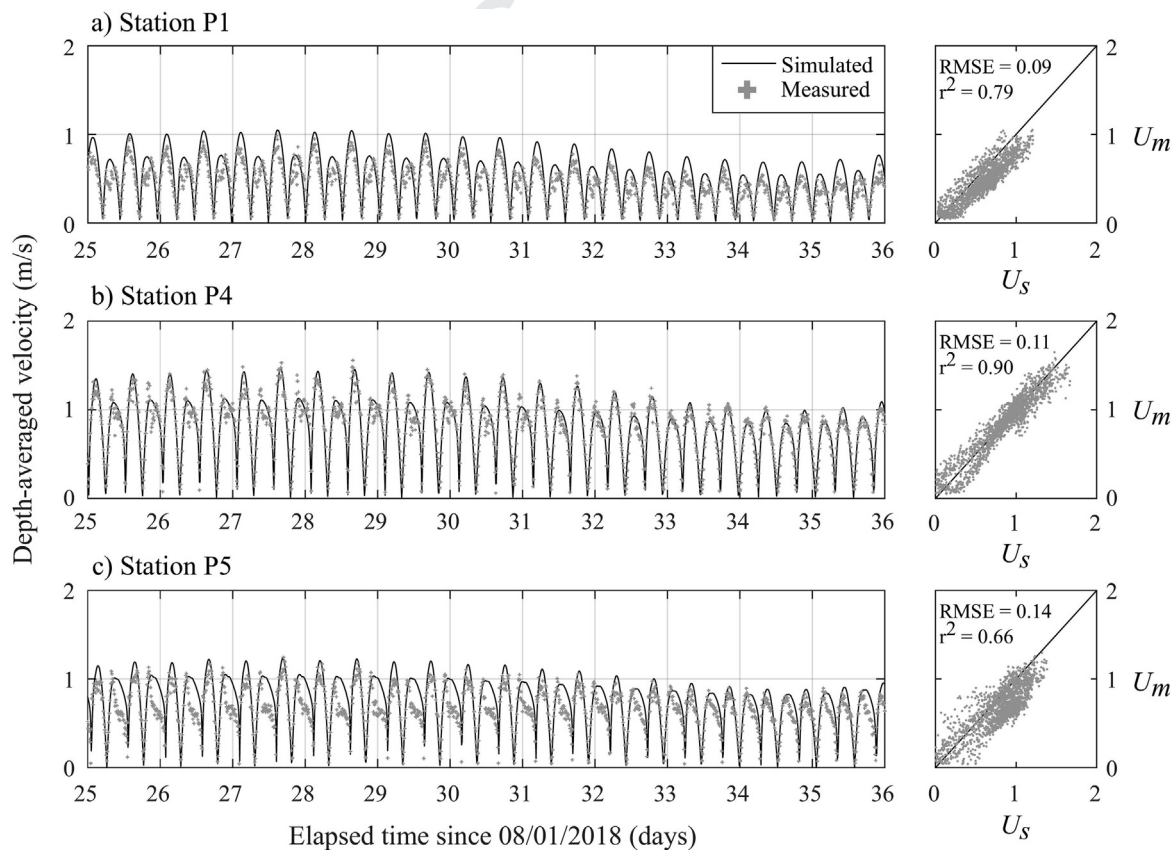


Fig. 5. Time series of simulated (black line) and measured (grey points) current velocities at stations (a) P1, (b) P4, and (c) P5 and their respective cross-validations. The simulation is done during a low river discharge period (from August to September 2018).

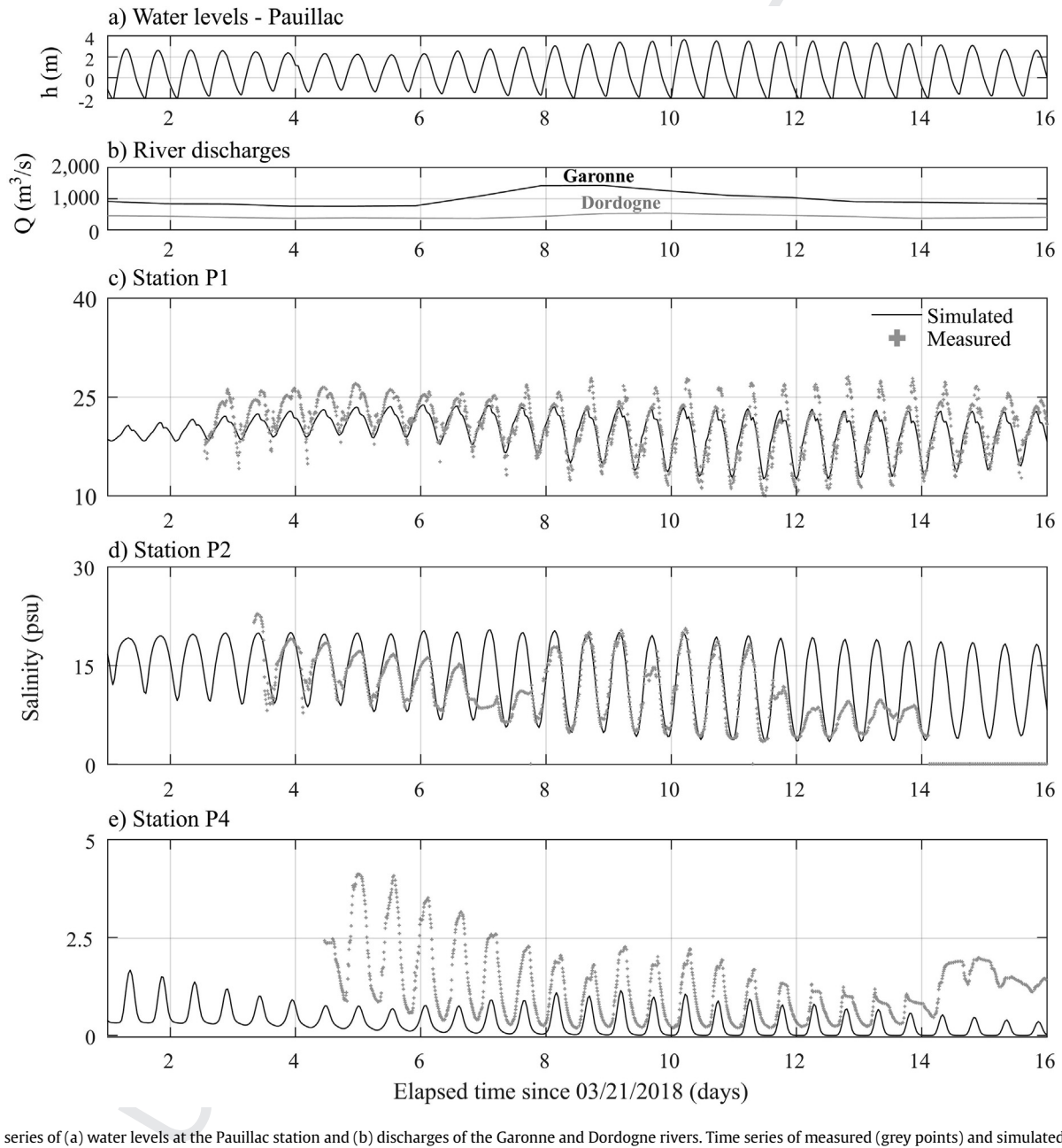


Fig. 6. Time series of (a) water levels at the Pauillac station and (b) discharges of the Garonne and Dordogne rivers. Time series of measured (grey points) and simulated (black line) depth-averaged salinity are shown for stations (c) P1, (d) P2, and (e) P4. The simulation is done during a high river discharge period (from March to April 2018).

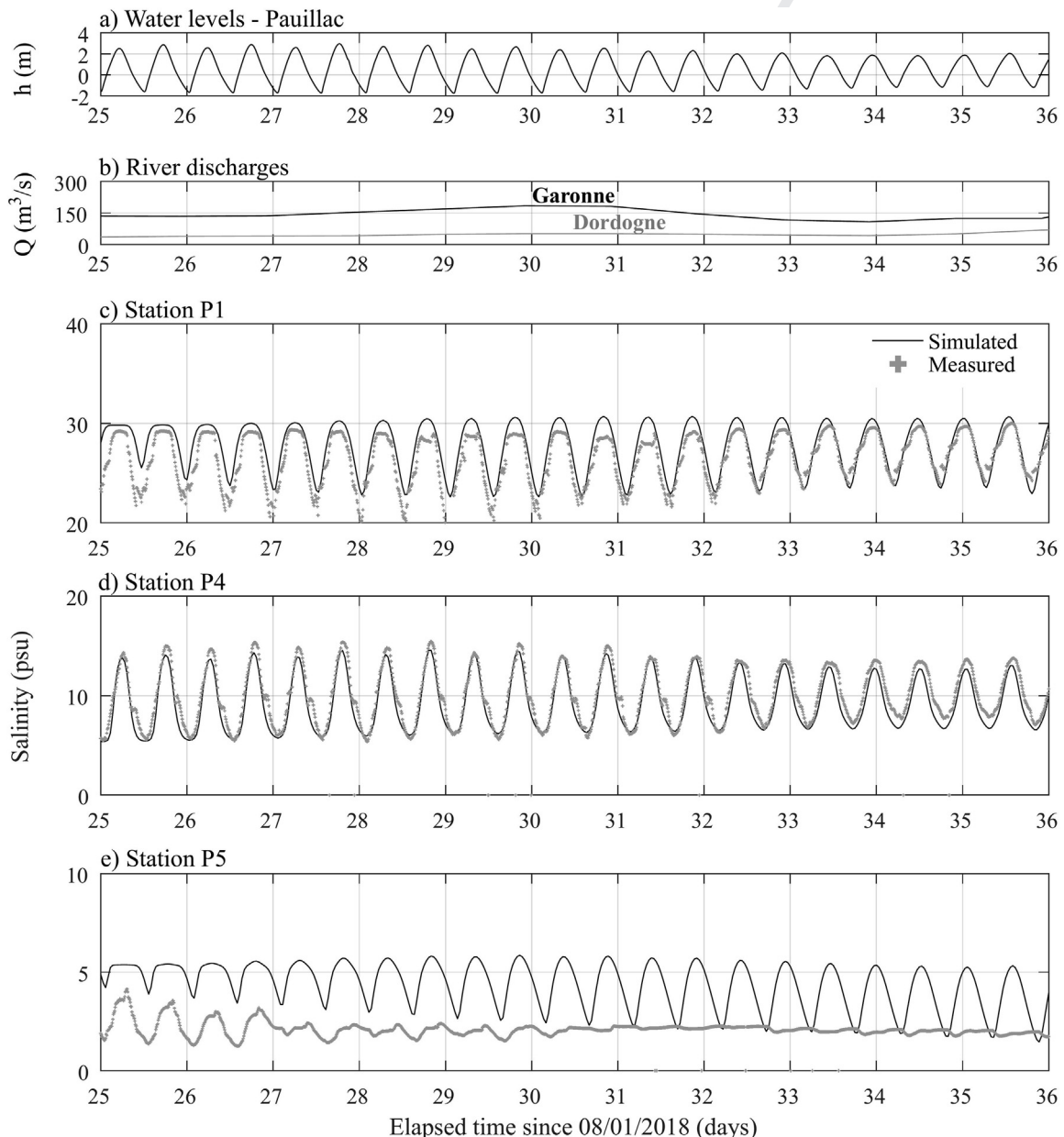


Fig. 7. Time series of (a) water levels at the Pauillac station and (b) discharges of the Garonne and Dordogne rivers. Time series of measured (grey points) and simulated (black line) depth-averaged salinity are shown for stations (c) P1, (d) P4, and (e) P5. The simulation is realized during a low river discharge period (from August to September 2018).

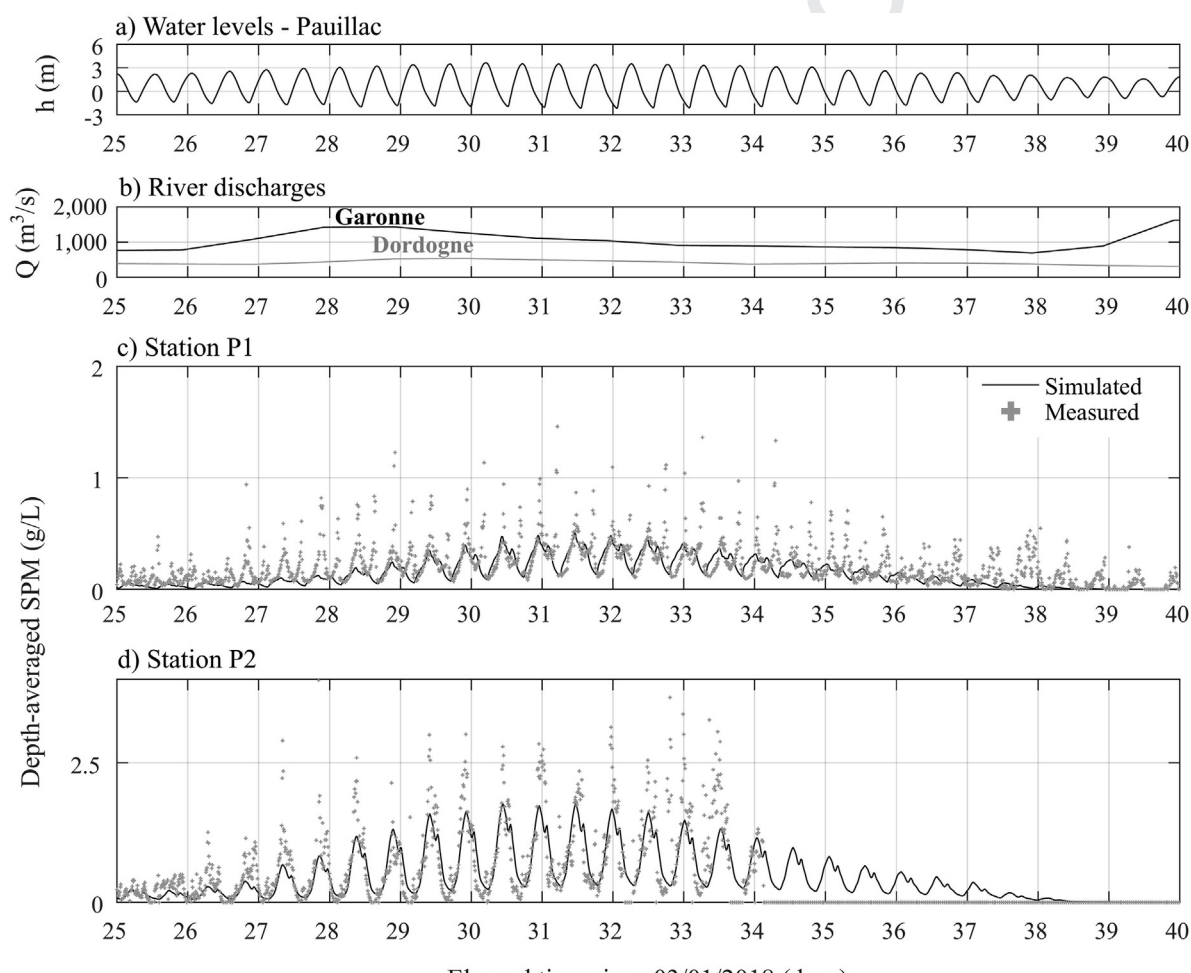


Fig. 8. Time series of (a) water levels at the Pauillac station and (b) discharges of the Garonne and Dordogne rivers. Time series of measured (grey points) and simulated (black line) depth-averaged SPM are shown for stations (c) P1, and (d) P2. The simulation is done during a high river discharge period (from March to April 2018).

period, only two stations were available due to the loss of a probe and the saturation of a sensor at the other one. Hydrological conditions are characterized by higher river discharge periods between days 26–28 and 39–40 (Fig. 8b). However, no clear relation appears with SPM due to the short duration of the simulation.

For both Stations P1 and P2, measured and simulated SPM are strongly related to the fortnightly cycle with maximum values observed during spring tides between days 30 and 34 (>3 g/L for measurements) and null values during neap tides at the end of the simulation (Fig. 8c and d). The dynamics of SPM is reliably predicted by the model excepted at the tidal scale. At this temporal scale, differences between ebb and flood maximum resuspension are not substantial, particularly at Station P1 (Fig. 8c). Although the model tends to underestimate SPM values for both stations, it provides reliable predictions for high river discharges.

During the simulation of low river discharges, flowrates are below 300 m³/s and spring and neap tides occurred during days 26–29 and 32–35, respectively. For these hydrological conditions, the TMZ migrates landward near Bordeaux inducing a decrease of SPM in the lower estuary, as observed at Station P2 (Fig. 9c). At this station, the model also accurately predicts the fortnightly dynamics, particularly during neap tides. As observed with high river discharges, tidal variations are still difficult to predict with no clear delineation between flood and ebb resuspensions. For Stations P4 and P5, SPM levels are clearly underestimated by the model by approximately 29 and 125%, respectively, and these underestimations could be explained by a combination of several factors (Fig. 9d and e). First, the model experiences some difficulties to keep suspended particles in the numerical domain over time due to deposition in shallow areas. Second, the numerical reproduction

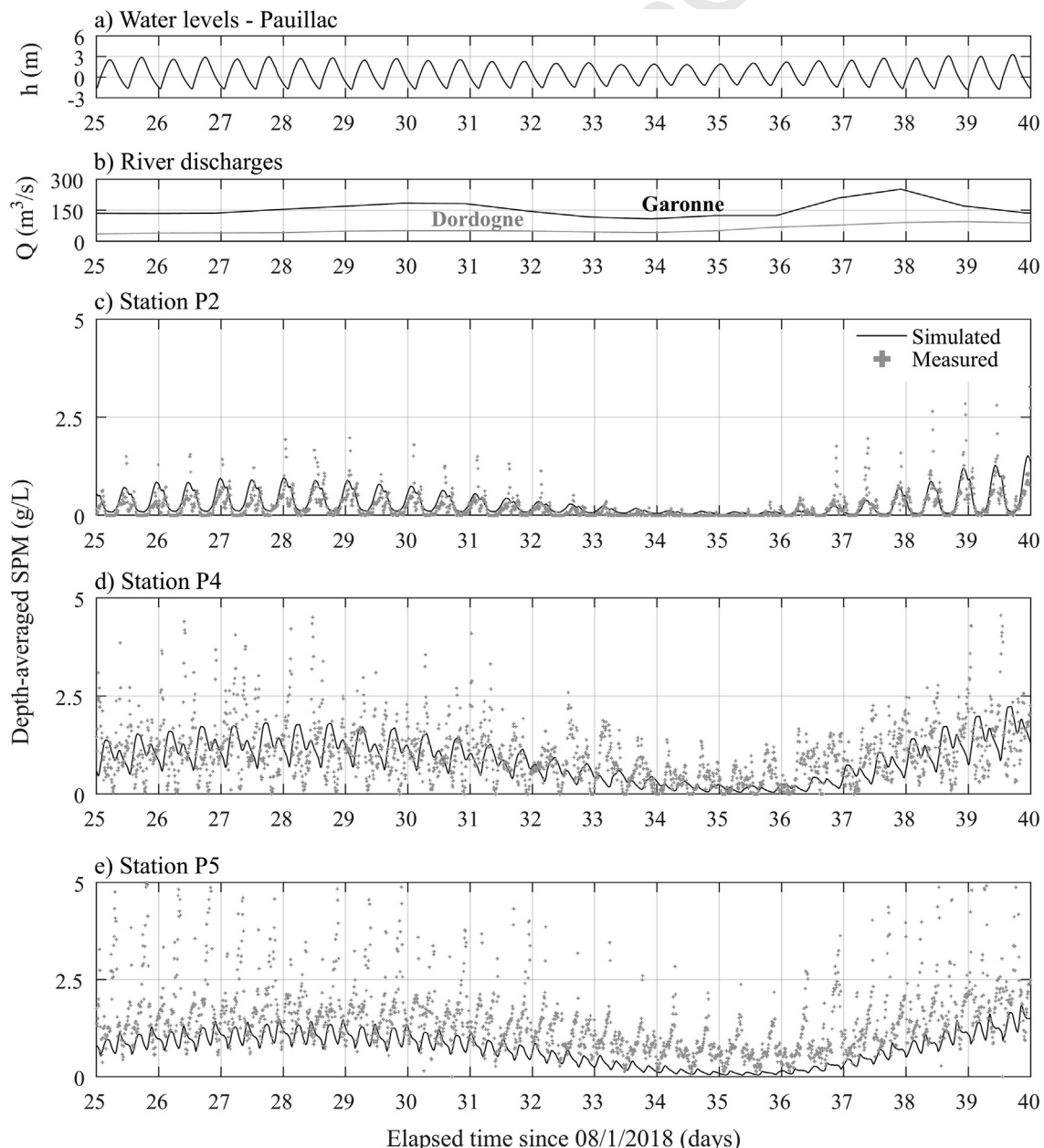


Fig. 9. Time series of (a) water levels at the Pauillac station and (b) discharges of the Garonne and Dordogne rivers. Time series of measured (grey points) and simulated (black line) depth-averaged SPM are shown for stations (c) P1, (d) P4, and (e) P5. The simulation is realized during a low river discharge period (from August to September 2018).

of the TMZ with a 2DH model does not consider the influence of vertical density gradients which act to maintain high suspended-sediment concentrations above the bed.

5. Sensitivity analysis

A sensitivity analysis is performed to study the influence of several physical parameters such as the critical shear stress for erosion, the settling velocity, the consolidation on depth-averaged SPM (Fig. 10) and fluid mud thickness (Fig. 11). The latter parameter corresponds to the sum of the first five layers (<150 g/L). Results are extracted from the intermediate estuary near the Pauillac station (Fig. 1). For the initial configuration, constant values are chosen for the settling velocity ($W_s = 0.75$ mm/s), the critical shear velocity for deposition ($u_{cd}^* = 10$ m/s) and the Partheniades constant ($M = 2 \times 10^{-3}$ kg/m²/s). For the erosion law, a linear relation between the critical shear stress and the mud layer concentration is considered (Section 3.1). This choice of relation is similar to those selected by van Maanen and Sottolichio (2018).

The first test compares the influence of erosion parameters: the critical shear stress for erosion and the Partheniades constant (Fig. 10a). Reducing of 20% the critical shear for erosion yields an increase in SPM of 73% and amplifies tidal variations. Conversely,

halving the Partheniades constant induces an overall decrease of SPM of 53% and expands the availability of sediment for consolidation increasing the thickness of the fluid mud layer (Fig. 11a).

Similar trends are observed with bed parameters including one simulation without bed consolidation and one simulation with the presence of sand in the intermediate estuary (Fig. 10c). As expected, without bed consolidation SPM concentrations increase and the fluid mud thickness becomes thicker (Fig. 11d). During the first month of the simulation, the fluid mud layer firstly becomes thinner until the mud deposit is completely resuspended and reaches an equilibrium on day 30 (Fig. 11d). However, for simulations covering a period of time of few months, fluid mud deposits in shallow areas are overestimated and reached unrealistic values (>5 m). For short-term simulations (up to 36 h), consolidation processes can be neglected. Fig. 10c also shows the strong influence of the assumption of the sand content. The addition of sand (10% per layer) in the intermediate estuary increases the critical shear stress for erosion, and, therefore, reduces resuspension. Moreover due to consolidation, the fluid mud is transferred to more consolidated layers which tends to increase the sand influence on the first layers. However, imposing 10% of sand in the intermediate estuary and in the entire mud substrate does not seem realistic. Sand is probably located around some banks or between muddy layers which may

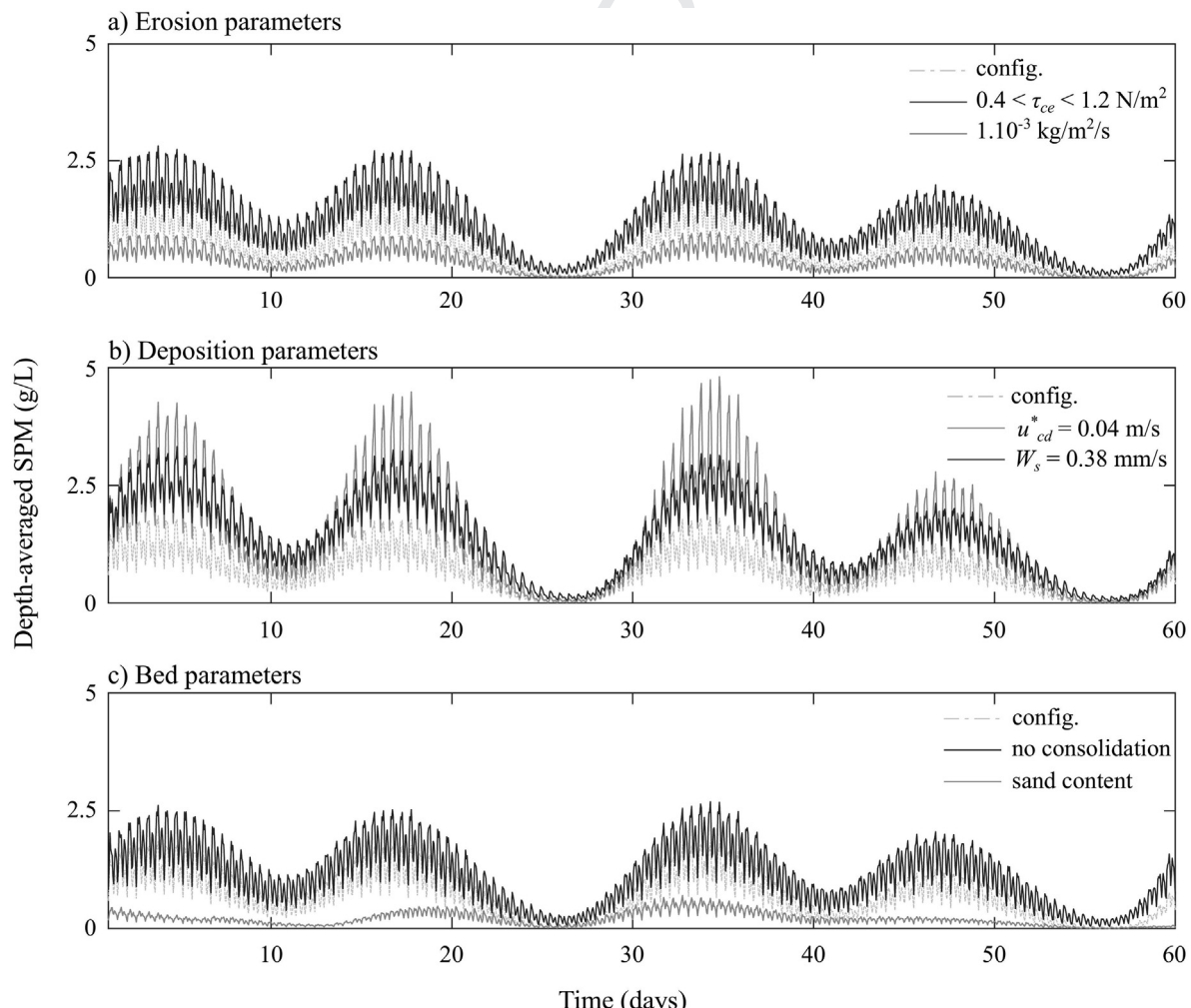


Fig. 10. Time series of depth-averaged suspended particulate matter (SPM) computed by the numerical model with different settings for (a) the critical shear stress for erosion (τ_{ce}) and the Partheniades constant (M), (b) the critical shear velocity for deposition (u_{cd}^*) and the settling velocity (W_s) and (c) without consolidation and depending on the sand fraction. Numerical results were extracted near the Pauillac station (Fig. 1) for a period of 60 days.

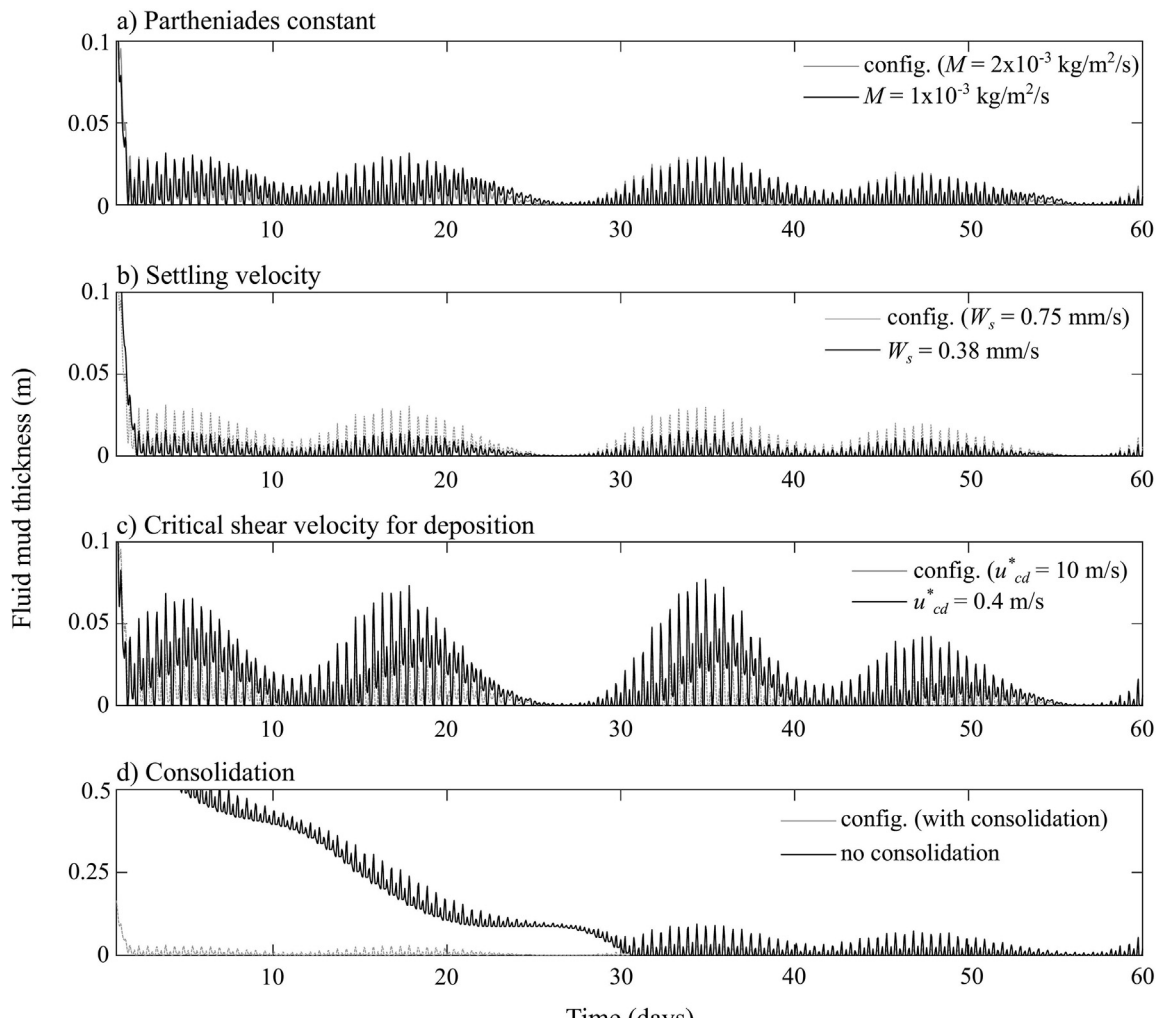


Fig. 11. Time series of the fluid mud thickness computed by the numerical model with different settings for (a) the Partheniades constant (M), (b) the settling velocity (W_s), (c) the critical shear velocity for deposition (u_{cd}^*), and (d) the consolidation. Numerical results were extracted near the Pauillac station for a period of 60 days.

be exposed to sediment transport according to the turbidity maximum migration or dredging activities. This result points out the importance of monitoring spatial and temporal variations of the bed material composition in order to provide reliable inputs for the model.

The last comparisons check the influence of two deposition parameters: the critical shear velocity for deposition and the settling velocity. Reducing by a factor of two these parameters leads to higher suspended-sediment concentrations up to 4.8 g/LI^{-1} and higher tidal variations (Fig. 10b). However, for the settling velocity no significant differences are noticed in fluid mud deposits since the deposition flux is proportional to the concentration of suspended sediment and the settling velocity (Fig. 11b). For the critical shear velocity for deposition, the fluid mud thickness reaches values up to 7–8 cm whereas it reaches 1–2 cm with the baseline simulation (Fig. 11c). A more energetic exchange, thus, is observed between the mud layer and the water column.

This parametric study illustrates the sensitivity of the model to the values of sediment parameters. These values are mostly imposed as constants over the computational domain. For the settling velocity it could be interesting to add spatial and temporal variability considering the influence of the suspended-sediment concentration. Similar improvement can be made for the critical

shear stress for deposition according to the transport capacity, as suggested by Bi and Toorman (2015).

6. Conclusions

The purpose of this paper is to develop a mixed sediment transport model for the prediction of the under keel clearance in the Gironde Estuary. The current study allows the hydrodynamics and sediment transport to be set up and validated with good accuracy. The harmonic analysis of the astronomical tides reveals (i) a strong distortion of the tidal wave inducing the growth of overtides constituents and (ii) the non-significant effect of tide-surge interactions for annual-scale predictions. Transport for sand-mud mixtures is considered for erosion, deposition, and consolidation processes with two sediment classes (sand and mud) and as a function of the mud fraction. Overall simulations were done with a fixed bed to validate suspended-sediment dynamics. The model was firstly validated for hydrodynamics by comparison with measured water levels and current velocities with high coefficients of determination. Predictions of salinity values also are reliable but show some deviations when the river discharge increases abruptly. Strong vertical density gradients also can explain observed differences. Suspended-sediment concentrations are correctly predicted

during flood conditions, but with a less-marked tidal dynamic. When river discharges are low, the model underestimates SPM levels probably due to the difficulty to maintain the TMZ without vertical density gradients. The sensitivity analysis has revealed a strong influence of (i) the settling velocity (ii) the critical shear stress for deposition, and (iii) the chosen erosion parameter for the computation of suspended-sediment concentrations and mud layer thicknesses in the intermediate estuary. This model will be used in the near future to compute the bed morphological changes and analyze the influence of bed load and suspended load transport and dredging/dumping operations in the navigation channel.

Declaration of Competing Interest

The manuscript has not been published and is not under consideration for publication in any other journal, All authors have approved the manuscript and its submission to the journal.

The authors whose names are listed in this manuscript certify that they have no affiliations with or involvement in any organization with any financial interest in the subject matter or materials discussed in this manuscript.

Acknowledgments

The research leading to these results has received funding from the Connecting Europe Facility (CEF) – Transport Sector under agreement (Innovation and Networks Executive Agency) No. INEA/CEF/TRAN/M2014/1049680 through the project Gironde XL. The authors thank the national hydrographic service (SHOM) for providing bathymetric datasets.

References

Abril, G., Riou, S. A., Etcheber, H., Frankignoulle, M., de Wit, R., & Middelburg, J. J. (2000). Transient, tidal time-scale, nitrogen transformations in an estuarine turbidity maximum-fluid mud system (The Gironde, South-west France). *Estuarine, Coastal and Shelf Science*, 50, 703–715.

Ali, M., Kaidi, S., & Lefrançois, E. (2018). Effect of the muddy area on the surface wave attenuation and the ship's squat. In *Lilamce 2018 congress*. November 11–14 2018, Paris/Compiègne, France.

Allen, G. P. (1972). *Etude des processus sédimentaires dans l'estuaire de la Gironde* (Ph.D. dissertation). University of Bordeaux I. (In French)

Bi, Q., & Toorman, E. A. (2015). Mixed-sediment transport modelling in Scheldt estuary with a physics-based bottom friction law. *Ocean Dynamics*, 65(4), 555–587.

Cancino, L., & Neves, R. (1999). Hydrodynamic and sediment suspension modelling in estuarine systems. Part II: Application to the Western Scheldt and Gironde estuaries. *Journal of Marine Systems*, 22(2–3), 117–131.

Castaing, P. (1981). *Le transfert à l'océan des suspensions estuariennes – Cas de la Gironde* (Ph.D. dissertation) (p. 530). Dept. University of Bordeaux I. (In French)

Chini, N., & Villaret, N. (2007). *Modélisation numérique hydro-sédimentaire de l'estuaire de la Gironde*. Thèse de DRT, Rapport interne EDF H-P73-2007-02094-FR, Chatou, France (p. 75). (In French)

Denot, T., Dribault, P., Boulet, T., & Courcier, P. (2000). *CNPE du Blayais, modélisation hydrodynamique 2D de l'estuaire de la Gironde avec prise en compte des zones de débordement*. Rapport EDF HP-72/2000/038/B, Chatou, France. (In French)

Diaz, M., Grasso, F., Le Hir, P., Caillaud, M., & Thouvenin, B. (2018). Numerical modelling of sediment exchanges from the Gironde estuary to the continental shelf: Sensitivity analysis of sediment transport parameters on sediment fluxes. In *Proceedings 6th international conference on estuaries and coasts: "Estuaries and coasts in times of global change"*. August 20–23 2018, Caen, France.

Hervouet, J. M. (2007). *Hydrodynamics of free surface flows modelling with the finite element method*. Chichester, UK: Wiley.

Huybrechts, N., & Villaret, C. (2013). Large-scale morphodynamic modelling of the Gironde Estuary, France. *Proceedings of the ICE - Maritime Engineering*, 166(2), 51–62.

Huybrechts, N., Villaret, C., & Lyard, F. (2012). Optimized predictive 2D hydrodynamic model of the Gironde Estuary (France). *Journal of Waterway, Port, Coastal, and Ocean Engineering*, 138(4), 312–322.

Jalón-Rojas, I., Schmidt, S., & Sottolichio, A. (2015). Turbidity in the fluvial Gironde Estuary (southwest France) based on 10-year continuous monitoring: Sensitivity to hydrological conditions. *Hydrology and Earth System Sciences*, 19(6), 2805–2819.

Jalón-Rojas, I., Sottolichio, A., Hanquiez, V., Fort, A., & Schmidt, S. (2018). To what extent multidecadal changes in morphology and fluvial discharge impact tide in

a convergent (turbid) tidal river. *Journal of Geophysical Research: Oceans*, 123(5), 3241–3258.

Jouanneau, J. M., & Latouche, C. (1981). *The Gironde Estuary, contributions to sedimentology* (Vol. 10). Stuttgart: E. Schweizerbart'sche Verlagsbuchhandlung.

Kapsimalis, V., Massé, L., & Tastet, J. (2004). Tidal impact on modern sedimentary facies in the Gironde Estuary, southwestern France. In *Proceedings of the STRAEE workshop - journal of coastal research* (Vol. 41, pp. 1–11).

Krone, R. B. (1962). *Flume studies of the transport of sediment in estuarial shoaling processes*. Final Report. Berkeley: Hydraulic Engineering Laboratory and Sanitary Engineering Research Laboratory. University of California.

Laborie, V., Hissel, F., & Sergent, P. (2014). Impact of climate change on Gironde Estuary. *La Houille Blanche*, 6, 34–39.

Le Hir, P., Fitch, A., Jacinto, R. S., et al. (2001). Fine sediment transport and accumulations at the mouth of the Seine Estuary (France). *Estuaries*, 24(6), 950–963.

Li, Z. H., Nguyen, K. D., Brun-Cottan, J. C., & Martin, J. M. (1994). Numerical simulation of the turbidity maximum transport in the Gironde Estuary (France). *Oceanologica Acta*, 17, 479–500.

van Maanen, B., & Sottolichio, A. (2018). Hydro- and sediment dynamics in the Gironde Estuary (France): Sensitivity to seasonal variations in river inflow and sea level rise. *Continental Shelf Research*, 165, 37–50.

McAnally, W. H., Friedrichs, C., Hamilton, D., et al. (2007a). Management of fluid mud in estuaries, bays and lakes. I: Present state of understanding on character and behavior. *Journal of Hydraulic Engineering*, 133(1), 9–22.

McAnally, W. H., Kirby, R., Hodge, S. H., et al. (2016). Nautical depth for U.S. Navigable waterways: A review. *Journal of Waterway, Port, Coastal, and Ocean Engineering*, 142(2).

McAnally, W. H., Teeter, A., Schoelhamer, D., et al. (2007b). Management of fluid mud in estuaries, bays and lakes. II: Measurement, modelling and management. *Journal of Hydraulic Engineering*, 133(1), 23–38.

Mélières, F., & Martin, J. M. (1969). Les minéraux argileux dans l'estuaire de la Gironde. In *Bulletin du Groupe français des argiles* (Vol. 21, pp. 114–126). (In French)

Pairaud, I. L., Lyard, F., Auclair, F., Letellier, T., & Marsaleix, P. (2008). Dynamics of the semi-diurnal and quarter-diurnal tides in the Bay of Biscay. *Continental Shelf Research*, 28(10–11), 1294–1315.

Parthenades, E. (1965). Erosion and deposition of cohesive soils. *Journal of the Hydraulics Division, ASCE*, 91(HY1), 105–139.

Pawlowicz, R., Beardsley, B., & Lentz, S. (2002). Classical tidal harmonic analysis including error estimates in MATLAB using T_TIDE. *Computers & Geosciences*, 28, 929–937.

Ross, L., Valle-Levinson, A., Sottolichio, A., & Huybrechts, N. (2017). Lateral variability of subtidal flow at the mid-reaches of a macrotidal estuary. *Journal of Geophysical Research: Oceans*, 122(9), 7651–7673.

Santoro, P., Fossati, M., Tassi, P., Huybrechts, N., Pham Van Bang, D., & Piedra-Cueva, I. (2017). A coupled wave-current-sediment transport model for an estuarine system: Application to the Río de la Plata and Montevideo Bay. *Applied Mathematical Modelling*, 52, 107–130.

Smaoui, H., Zouhri, L., Kaidi, S., & Carlier, E. (2018). Combination of FEM and CMAE-ES algorithm for transmissivity identification in aquifer system. *Hydrological Processes*, 32(2), 264–277.

Sottolichio, A. (1999). *Modélisation de la dynamique des structures turbides (bouchon vaseux et crème de vase) dans l'estuaire de la Gironde* (Ph.D. dissertation). University of Bordeaux I. (In French)

Sottolichio, A., & Castaing, P. (1999). A synthesis on seasonal dynamics of highly-concentrated structures in the Gironde Estuary. *Comptes Rendus de l'Académie des Sciences*, 329, 795–800.

Sottolichio, A., Le Hir, P., & Castaing, P. (2001). Modelling mechanisms for the turbidity maximum stability in the Gironde Estuary, France. In W. H. McAnally, & A. J. Mehta (Eds.), *Proceedings in Marine Science - coastal and estuarine fine sediment processes* (Vol. 3, pp. 373–386). Amsterdam: Elsevier.

Thiebot, J., Guillou, S., & Brun-Cottan, J.-C. (2011). An optimisation method for determining permeability and effective stress relationships of consolidating cohesive sediment deposits. *Continental Shelf Research*, 31, 117–123.

Van, L. A. (2012). *Modélisation du transport des sédiments mixtes sable-vase et application à la morphodynamique de l'estuaire de la Gironde* (Ph.D. dissertation). Laboratoire Hydraulique Saint-Venant & University of Paris-Est, France. (In French)

Van Rijn, L. C. (2007). Unified view of sediment transport by currents and waves, I: Initiation of motion, bed roughness and bed-load transport. *Journal of Hydraulic Engineering*, 133(6), 649–667.

Villaret, C., Huybrechts, N., & Van, L. A. (2011). Large scale morphodynamic modeling of the Gironde Estuary. In X. Shao, Z. Wang, & C. Wang (Eds.), *Proceedings, 7th IAHR Symposium on river, Coastal and estuarine morphodynamics*. Sept. 6–8, 2011, Beijing China, 12p.

Villaret, C., Van, L. A., Huybrechts, N., Pham Van Bang, D., & Boucher, O. (2010). Consolidation effects on morphodynamics modelling: Application to the Gironde estuary. *La Houille Blanche*, 6, 15–24.

Villaret, C., & Walther, R. (2008). Numerical modeling of the morphodynamic evolution of the Gironde Estuary. In *Proceedings 14th physics of estuaries and coastal seas conference*. August 26–29, Liverpool, England.

Waeles, B. (2005). *Modélisation morphodynamique de l'embranchement de la Seine* (Ph.D. dissertation). University of Caen-Basse Normandie. (In French)

Xu, J., & Yuan, J. (2007). Study on the possibility of occurrence of fluid mud in the Yangtze deep waterway. In *Proceedings of the 5th international conference on estuaries and coasts* (pp. 516–520). Hangzhou, China.